DISTRIBUTION STATEMENT A. Approved for public release; distribution is unlimited.

Analysis of Riverine Skin Temperature Response to Surface and Subsurface Processes

Christopher J. Zappa
Lamont-Doherty Earth Observatory of Columbia University
Ocean and Climate Physics Division
61 Route 9W
Palisades, NY 10964
Phone: (845) 365-8547 fax: (845) 365-8157 email: zappa@ldeo.columbia.edu

Award Number : N00014-15-1-2153

LONG-TERM GOALS

The primary research goal is to develop techniques to determine subsurface turbulence from remote measurements using infrared imaging of the skin layer. We aim to use infrared imaging of water surface patterns to deliver remote measurements of flow rate and turbulence intensity, and information on surface- and subsurface-generated turbulent structures in rivers. We will take advantage of the two complementary indicators of subsurface flow provided by IR imagery: the thermal structures measured directly and the surface velocity fields obtained through various image processing techniques. At the core of this project is the continued analysis for three publications from our collaboration with Areté Associates on our Hudson River data sets from November 2010. We aim to:

1) Predict water depth from surface integral length scales of turbulence derived from autocorrelation functions of skin temperature from infrared imagery. (What do the scales of boils tell us!)
2) Quantify variability of and model skin temperature as a function of environmental forcing in riverine and estuarine systems. (When are boils observed and not!)
3) Quantify observations of wind gustiness in infrared imagery. (Changes in surface roughness can disrupt the surface thermal boundary layer. Changes in surface roughness can also change the emissivity at high incidence angles. Gustiness can also increase the local heat flux and the change the temperature gradient across surface thermal boundary layer. All may impact the IR signature due to gustiness.)

OBJECTIVES

The skin temperature is governed by surface and subsurface processes. Net air-water heat flux leads to a cooler thermal boundary layer (TBL) compared to the underlying bulk layer. Turbulent motions resulting from wind forcing at the air-sea interface and from turbulent eddies generated within the water column, disrupt the TBL, mixing it with the bulk layer. During the last century links between air-water transfer and bulk turbulence were researched [*Brumley and Jirka*, 1988; *Danckwerts*, 1951]. Only in the last decade, has the TBL been recognized as the intermediate step between subsurface turbulence and air-water transfer and as such was used as a more direct indicator for air-water transfer [*McKenna and McGillis*, 2004]. This study will use the TBL as a direct indicator for subsurface

turbulence and provide predictive relationships of the surface-bulk connection. It will result in a be a set of universal curves connecting remotely collected surface measurements to fundamental local flow quantities – the flow depth, the bed stress, the bulk mean flow and the bulk turbulent kinetic energy. We will (1) analyze the variability and structures of the thermal boundary layer, (2) compute the surface flow field from the IR imagery and infer further surface turbulence characteristics, (3) determine to which extent the turbulence in the boundary layer is due to surface forcing by analysis of the air-sea flux data and (4) determine empirical relationships of subsurface flow characteristics and of turbulence derived from in situ sub-surface data to the observed turbulence in the IR imagery. We further aim to determine the limits of remotely inferring flow rates, subsurface turbulence and bed stress from IR imagery. We will investigate how different wind, tides and wave breaking conditions affect our ability to remotely measure subsurface flow characteristics.

APPROACH

Surface measurements were performed with an IR camera, utilizing natural surface "seeding" provided by the spatial variance in the surface temperature field. This variance always exists as a result of the net air-water heat flux that causes temperature differences between the bulk and surface layers, and the turbulent motions that intermittently stir and mix these two layers. IR images demonstrate the technique's ability to resolve micro-scale features (see *Zappa et al.* [2003]) as well as large-scale features (see *Zappa and Jessup* [2005]), and clearly allow for airborne implementation.

IR images provide two complementary indicators of subsurface flow – instantaneous thermal structure measured in each image and surface velocity fields obtained from feature pattern matching of subsequent images. These surface flow measurements can be combined with an accounting of the surface features to determine velocity profiles as described below. Doing this requires interpreting surface patterns formed by the superposition of turbulent sources (bed stress and surface stress), convection (thermal and wind-driven, *e.g.* Langmuir cells) and advection (tidal and wind-driven). Furthermore, the capability of surveying at many scales requires that our phenomenology work at many resolutions. To address these challenges we chose an empirical approach. That is, we will develop and then use a series of parameterizations relating the observable IR surface fields to the hydrodynamic properties of interest – flow rate, subsurface turbulence, and bed stress. This empirical study will take place in the field on the Hudson River in New York.

Building on our extensive expertise in IR imagery and our experience in making near-boundary turbulence measurements, we aim to determine empirical relationships between surface length-scales and flow and sub-surface flow and turbulence. During the prototype field campaign, data was collected with the following instruments:

- <u>IR camera</u>: a Cedip Jade III longwave camera was mounted a pan/tilt system from the A-frame of a moored ship. This set up allowed us to move the camera with the current so to always view upstream of the ship. The Cedip Jade III offers better than 15 mK temperature resolution, with 200 Hz max frame rate, 14-bit digitization, and 320 x 240 pixels. The sampling frequency was set to 60 Hz.
- <u>Air-Sea Flux package:</u> a meteorological station was mounted on a piling neighbouring the ship to get measurements of wind speed & direction, relatively humidity, atmospheric pressure, air temperature, solar insolation, and longwave radiation.

- Acoustic Doppler Velocimeter (ADV): a Nortek Vector type ADV was mounted on the aforementioned piling at 11m above the River bed. Data was collected in 10 min bursts at top of every ½ hr, with a sampling frequency 32Hz.
- Higher Resolution Profilers: 2 Nortek Aquadopp were mounted on the piling at 3 and 6 m above the river bed. They offer a 1-cm resolution. Data was collected in 59.9 min burst at top of every hour, with a sampling frequency 2 Hz.
- CTDs: 3 CTDs were mounted on the piling at the same levels as the ADV and Aquadopps

The team's envisaged data analysis effort includes: image processing and analysis of the IR imagery to characterize surface turbulence. This comprises calculation of the statistical moments, histograms to assess surface skin temperature variability, and determination of length scales of the skin temperature structures. Further, 3 methods to determine the surface velocity field from the IR imagery will allow inferring integral length scales, as well as the surface turbulent kinetic energy and calculation of divergence. The bulk Reynolds number can then be determined from the divergence. Analysis of the Aquadopps, ADV and CTD data combined will provide a robust measure of subsurface turbulent, convective, and advective motions. Links between the subsurface and surface turbulence will be investigated, keeping in mind that the observed turbulence at the surface is partly due to surface forcing. Processing and analysis of the direct measurement of heat, mass and momentum fluxes across the air-water interface along with measurements of the radiative forcing will permit to separate the different processes (wind-driven, bed-driven, buoyancy-driven, and convective) which lead to surface turbulence.

WORK COMPLETED

Our efforts FY15 comprised image processing and analysis of IR imagery taken from the ship and analysis of in situ measurmeents so to address points (1) through (4) of the Objectives. Skin temperature variance was shown to decrease with increasing wind speend and latent heat flux. Surface integral length scales were determined from the skin temperature and are shown to be linearly related to water column depth. Surface currents were derived via three algorithms: Digital Particle Image Velocimetry, Optical Flow and Spectral Advective Surface. They gave estimates that were highly correlated to the subsurface flow measurements with comparable 10 minute mean magnitudes. We have presented our results at the AGU Fall Meeting, San Francisco, CA, USA in December 2011 [*Zuckerman et al.*, 2011] and 2012 [*Brumer et al.*, 2012]. We have submitted a manucript that covers these Objectives and is currently in its 2nd revision. The manuscript describes the characteristic surface length scale determined from IR imagery and its relationship to water depth and turbulent dissipation rates. The highlights are described below.

RESULTS

Environmental conditions including surface and subsurface currents

IR measurements were taken under varying wind conditions, with 20 minute average 10-m neutral wind speed ranged from 0.29 m s^{-1} to 4.01 m s^{-1}. The 10-m neutral wind speed averaged 3.15 ± 0.74 m s^{-1} on the night of the 18th (yearday 322) and 1.2 ± 0.61m s^{-1} on the night of the 19th (yearday 323). As a result, the momentum flux was much stronger on the 18th with a mean and standard deviation of 0.30 ± 0.23 kg m^{-1} s^{-2}; on the 19th it only reached 0.13 ± 0.08 kg m^{-1} s^{-2}.

Measurements coincided with the ebbing tide on the first night and low water to flood tide during the second night. An estimate of the bulk current speed was obtained by computing a column averaged velocity from the ADCP from the deepest bin to the top good bin about 50-75 cm below the water surface. Over the period time IR imagery was recorded, the 10-minute averaged current speed measured by the ADCP ranged from 0.07 m s^{-1} to 0.73 m s^{-1}. These strongly correlated to the 10 minute average ADV measurements (r^2=0.9, cf. Figure 1a). We simultaneously used 2 approaches to determine surface velocity fields:

1. Feature tracking or Digital Particle Image Velocimetry (DPIV; e.g. *McKenna and McGillis* [2002], *Variano and Cowen* [2008])
2. Spectral Advective Surface (SAS) in 3D spectra of the skin temperature [*Dugan and Piotrowski*, 2012]

to investigate both the bulk flow (which we wish to parameterize) and the near-surface region (where the physics responsible for translating bulk motions into surface motions occurs). Even though one would expect the surface flow to be wind driven, the winds experienced were so weak that the surface velocities derived from the imagery match the column averaged ADCP (r^2=0.89 for SAS and r^2= 0.82 for DPIV, cf. Figure 1b and c) velocities and ADV velocities (r^2 = 0.79 for SAS and r^2= 0.71 for DPIV). The surface velocities were also found to correlate with the bottom ADCP measurements (r^2=0.78 for SAS and r^2= 0.68 for DPIV). Both surface current retrieval methods agree very well with an r^2 = 0.95.

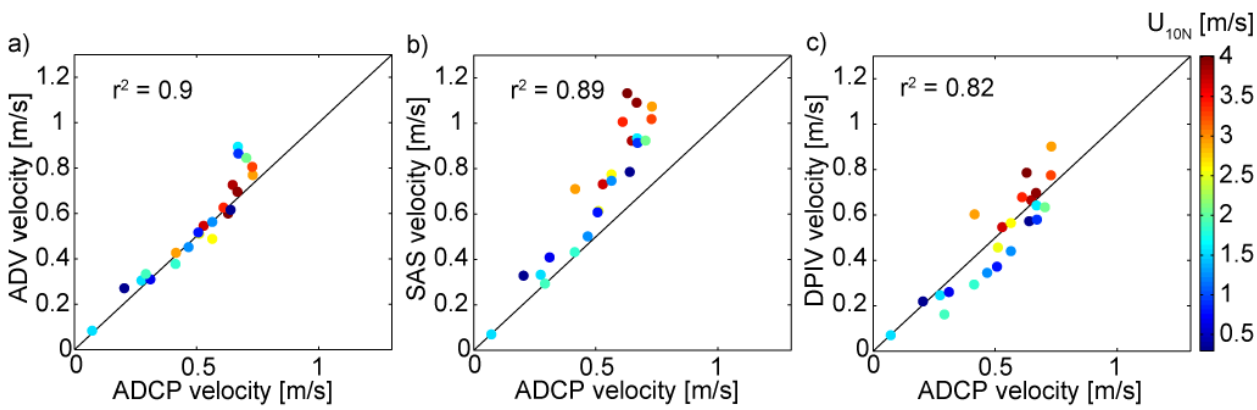

Figure 1. Scatter plots of the run mean flow magnitudes derived from the a) ADCP against the ADV, b) ADCP vs. DPIV and c) ADCP vs. SAS. The data are color-coded according to the 10-m neutral wind speed (U_{10N}). The 1:1 line is shown in black.

Correlation coefficients do not provide sufficient information to conclude on how imagery derived flows compare to measured subsurface flows as it only provides an insight on how closely they are linearly related, but says nothing about how they compare in actual magnitude. The scatter plots (c.f. Figure 1b and c) clearly show that not only are they well correlated, but they are also of comparable magnitude.

Turbulent kinetic energy dissipation

The turbulent kinetic energy (TKE) dissipation rate ϵ can be estimated by fitting the inertial subrange of wavenumber spectra ($\Phi(k)$) with a $k^{-5/3}$ slope following the Kolmogorov turbulence cascades which dictates that:

$$\Phi(k) = \alpha\epsilon^{\frac{2}{3}}k^{-\frac{5}{3}}$$

where k denotes the wavenumber and α is a constant. Wavenumber spectra can be computed directly from the IR derived velocity fields or Aquadopp profiles. However, for time series measurement of velocities such as collected by ADVs, it is necessary to make a further assumption in order to derive TKE dissipation rates. Assuming that the frozen Taylor hypothesis is valid, i.e. that turbulent eddies remain unchanged while being advected by the mean flow, one can convert frequency spectra $S(f)$ into wavenumber spectra as follows:

$$\Phi(k) = S(f).\frac{\langle v\rangle}{2\pi}, \text{ with } k = 2\pi f/\langle v\rangle$$

where f is the frequency and $\langle v\rangle$ the mean velocity.

Surface derived TKE dissipation rates correlate with the subsurface dissipation rates (cf. Figure 2). Both DPIV and Aquadopp TKE dissipation rates were computed directly from wavenumber spectra, whereas the ADV TKE dissipation rates were derived from frequency spectra assuming the validity of the Taylor hypothesis of frozen flow. All runs with reflection have been discarded since they generate unreliable DPIV fields. The linear correlation coefficient is 0.59 between the surface $\boldsymbol{\varepsilon}$ and the ADV $\boldsymbol{\varepsilon}$ and 0.75 between the surface $\boldsymbol{\varepsilon}$ and the Aquadopp mounted at 0.91 m above the river bed. The correlation coefficient between the surface $\boldsymbol{\varepsilon}$ and the Aquadopp mounted at 1.83 m above the surface is of 0.33.The strong correlation throughout the water column is expected due to the low stratification and low wind conditions.

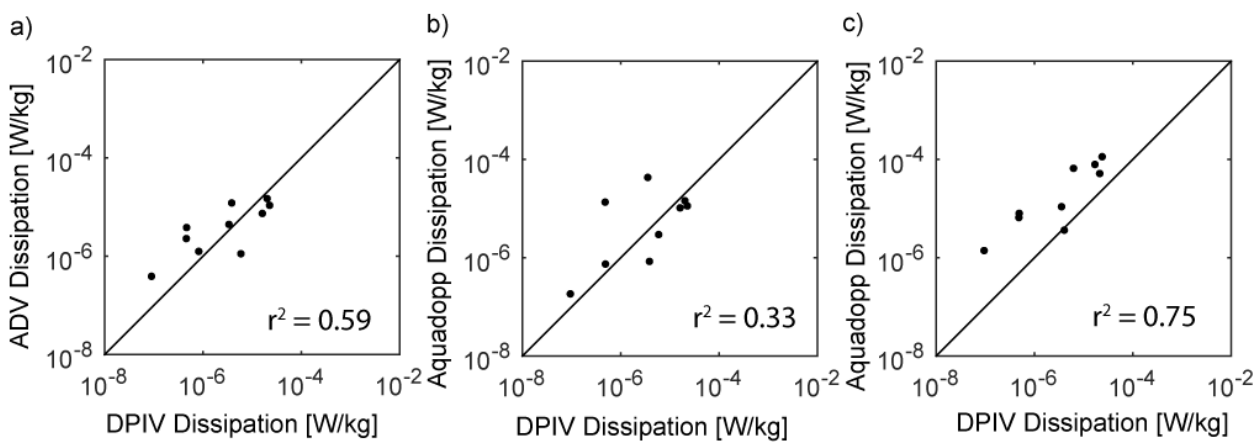

Figure 2. DPIV derived TKE dissipation rates versus a) that from the ADV at 3.35 m above the river bed, b) that from the bottom Aquadopp at 1.83 m above the river bed, and c) that from the bottom Aquadopp at 0.91 m above the river bed. The 1:1 line is shown in black.

Surface length scale determined from imagery and correlation with depth

Characteristic surface length scales are determined directly from the skin temperature imagery and from the DPIV velocity fields from which the frame mean velocity was removed. In order to do so, it is necessary to scale the imagery and transform the camera coordinates to water level coordinates. This is achieved through a rotation matrix using the roll, pitch, and yaw angles measured by the IMU as exemplified in Figure 3.

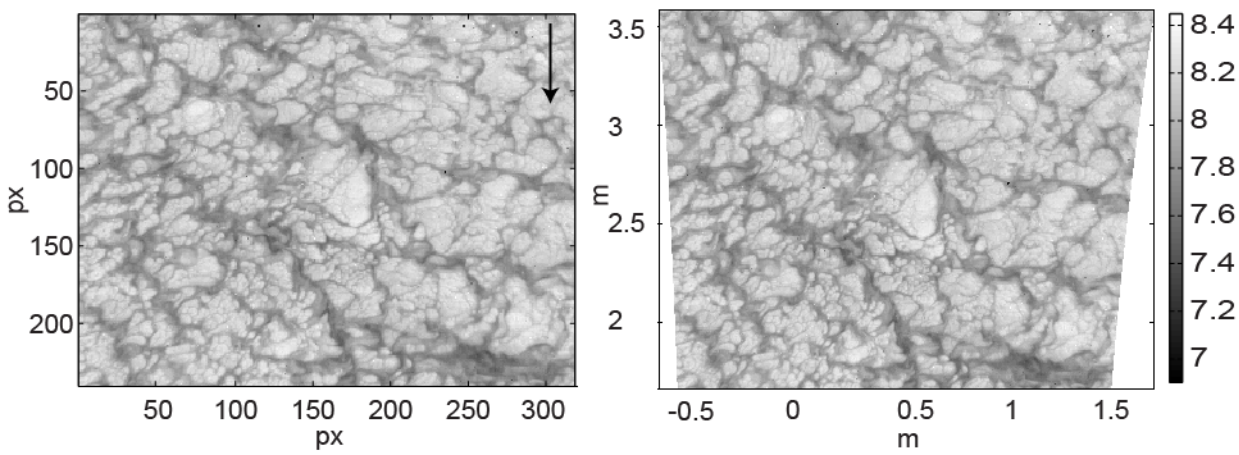

Figure 3. a) An example of a calibrated IR image pre-projection correction; the black arrow indicates the mean flow direction. b) The same fame scaled and projected correctly

From the scaled fields, normalized auto-covariance functions were computed for each row and column of each frame (an example of which is shown in Figure 4). The normalized auto-covariance is given by: $C_{XX}(\mathrm{r}) = \frac{\sum_{i=0}^{N-r} x(i)x(i+r)}{\sum_{i=0}^{N} x(i)^2}$, where r is the lag, N is the number of pixel in a row or column and $x(i)$ is the temperature of a given pixel. For each frame, two mean normalized auto-covariance functions were subsequently computed, one for each dimension. Characteristic skin temperature length scales (L1 and L2) were determined as the distance at which the skin temperatures are no longer correlated, i.e. corresponding to the smallest lag at which the frame mean auto-covariance function are equal to zero. From the DPIV fields we first computed 4 length scales, one for each component of the velocity vector for both dimensions of the image which were averaged to give one single scale for each run.

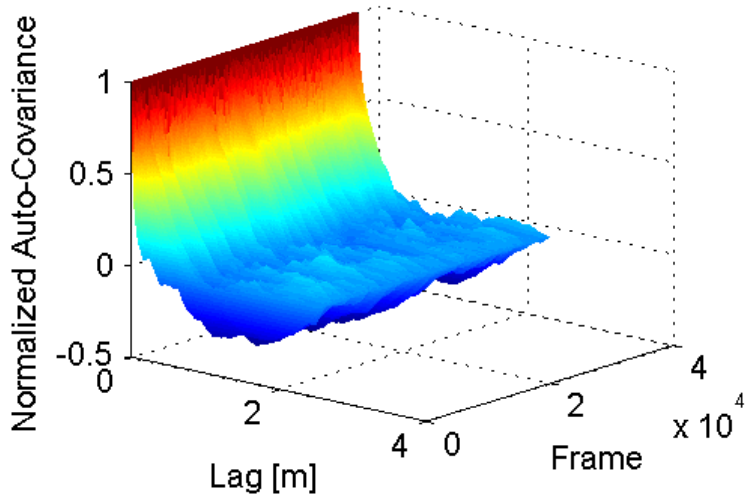

Figure 4. Sample time series of the frame averaged normalized spatial auto-covariance of the thermal imagery for various lags

As seen in Figure 3, the river surface is covered by warm features, depicted in lighter gray, surrounded by colder, darker filaments. The warm skin temperatures result from bulk water brought to the surface. The scale of these macro turbulent features seem to remain relatively constant over the duration of the 10 minute runs allowing for surface length scales to be defined. The warm features are slightly anisotropic, often elongated in the direction of the flow. In some videos taken during the first night, reflection from the A-frame can be seen in the imagery as a cold artifact. These videos coincide with the period of time when the water column was more stratified and winds were stronger as noted in the previous section and are excluded from the subsequent analysis purely based on the presence of reflection.

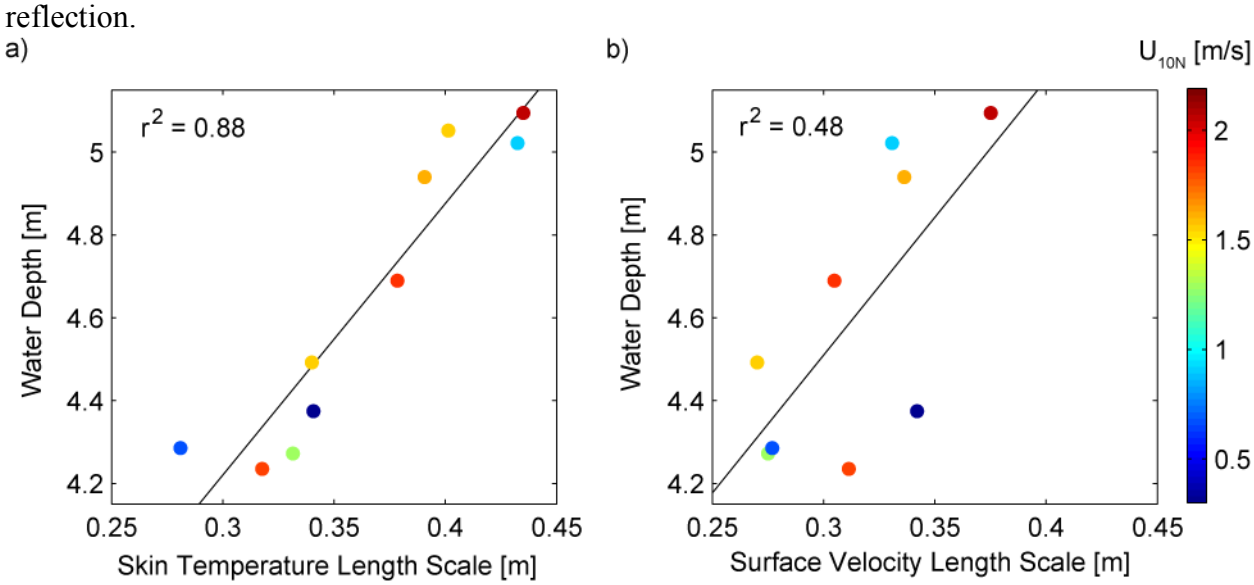

Figure 5. Scatter plot of the surface scales derived from the spatial autocorrelation functions of a) the skin temperature and b) the DPIV velocity fields against height of the water column. The dots are color-coded according to the 10-m neutral wind speed (U_{10N}) and the black line shows the linear fit

For each run, a mean length scale was computed from L1 and L2. Figure 5a shows a scatter plot of the length scales derived from the skin temperature fields versus water depth. The results show the scale of the surface features (**L**) is strongly linearly correlated (r^2=0.88) to the water depth (**D**), with a slope of **D/ L** ~ 13. Outliers, excluded from the figure and the fit, correspond to the runs when the water column reflections dominated the temperature field. The correlation is slightly stronger (r^2=0.93) with L2 which roughly corresponds to the direction of flow and weakly correlated with L1 (r^2=0.37).

Although the mean length scale derived from the DPIV increases with water depth (cf. Figure 5b), the linear correlation is much smaller (r^2=0.48). On average the mean DPIV scales are found to differ by ~7 cm from the temperature scales. This can mostly be attributed to the difference in resolution of the fields used to determine the scales. Indeed, the temperature scale has a pixel resolution i.e. ~0.8 cm whereas the scale derived from the DPIV has a resolution of ~6.4 cm.

Determining subsurface dissipation rates from surface current and surface length scales

The turbulent kinetic energy dissipation rate can be estimated from the both the flow speed (***U***) and the dominant length scale in the flow (***L***). On the one hand, the dissipation rate equals the kinetic energy production rate which is proportional to $\boldsymbol{U}^2$. One the other hand, the rate of kinetic energy supply can be thought as proportional to the inverse turnover time of large eddies: $\boldsymbol{L}/\boldsymbol{U}$. This implies $\varepsilon \sim \frac{U^2}{L/U} \sim \frac{U^3}{L}$ [*Tennekes and Lumley*, 1972]. As seen in figure 6, $\frac{U^3}{L}$ computed from surface length scales and surface currents is highly linearly correlated to ϵ derive from the Aquadopp. Correlations are the strongest when using SAS velocities (r^2 = 0.9) and slightly lower when using DPIV (r^2 = 0.82) velocities. The strength of the correlation is comparable when the length scales derived directly from the temperature field or derived from the DPIV are used. Since the surface length scales ***L*** are highly correlated to ***D*** (see figure 5) the correlations are comparable. Using DPIV mean flow we get r^2 = 0.8 and using SAS mean flow we get r^2 = 0.86.

IMPACT/APPLICATIONS

Although in this field campaign the IR remote sensing was performed from a ship, the analysis and results obtained in this study should be easily adaptable to imagery taken from other platforms such as aircrafts, manned and unmanned, as well as fixed platforms. This study reinforces the idea that IR remote sensing is an excellent surveying tool for estuarine environments and encourages continued research in the field. The strong linear relation between depth and surface integral length scales derived from the temperature fields may provide a useful method to estimate bathymetry, especially when no waves are present.

The good agreement between the IR derived and sub-surface TKE dissipation estimates reinforces the adequacy of IR remote sensing for studies of estuarine and riverine turbulence. Previous studies have already shown how IR derived dissipation rates reflects in situ measured dissipation well [e.g., *Chickadel et al.*, 2011]. Unlike us, they made use of the Taylor hypothesis even for the imagery estimates, choosing to compute dissipation at a single location.

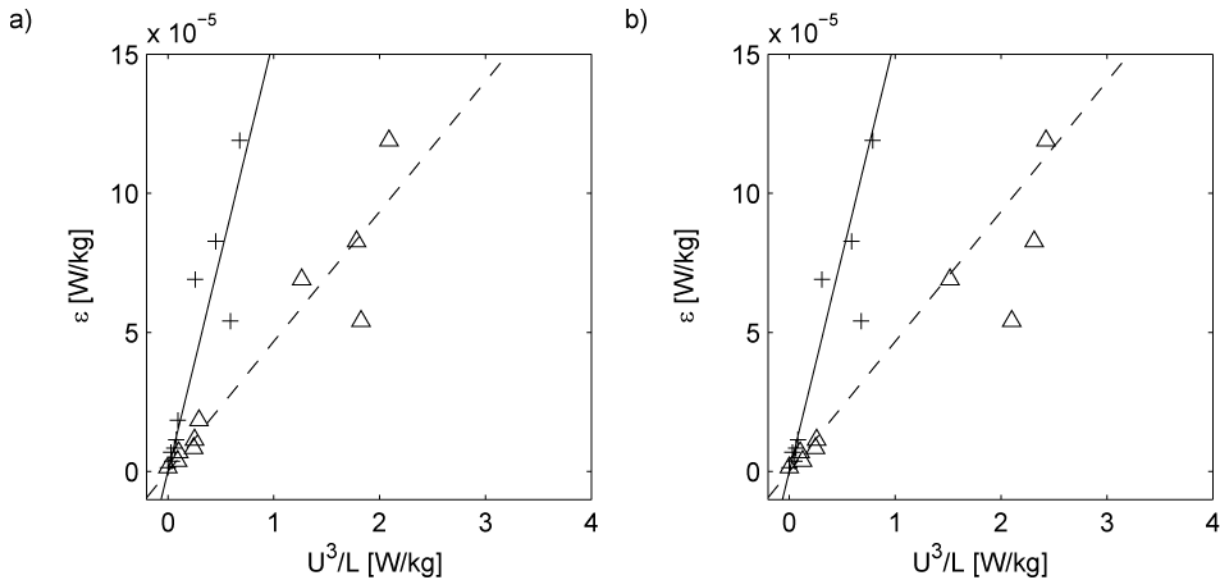

Figure 6. Scatter plots of the dissipation measured by the bottom Aquadopp against U^3/L where U is the mean velocity derived from the SAS (Δ) and DPIV (+) and L is the temperature length scale in a) and the DPIV scale in b). The solid and dashed lines show the best fit of the form y = a × x when using the DPIV and SAS velocity respectively. The proportionality coefficient or slope to the best fit in a) is 4.7×10^{-5} for SAS and 1.6×10^{-4} for DPIV and in b) 3.9×10^{-6} for SAS and 1×10^{-4} for DPIV

REFERENCES

Brumer, S. E., C. J. Zappa, S. P. Anderson, and J. P. Dugan (2012), Using skin temperature variability to quantify surface and subsurface estuarine processes, *AGU Fall Meeting Abstracts*, *14*, 05.

Brumley, B. H., and G. H. Jirka (1988), Air-water transfer of slightly soluble gases: Turbulence, interfacial processes and conceptual models, *PhysicoChemical Hydrodynamics*, *10*(3), 295-319.

Chickadel, C. C., S. A. Talke, A. R. Horner-Devine, and A. T. Jessup (2011), Infrared-based measurements of velocity, turbulent kinetic energy, and dissipation at the water surface in a tidal river, *IEEE Geoscience and Remote Sensing Letters*, *8*(5), 849-853, doi:10.1109/LGRS.2011.2125942.

Danckwerts, P. V. (1951), Significance of liquid-film coefficients in gas absorption, *Industrial and Engineering Chemistry*, *43*(6), 1460-1467.

Dugan, J. P., and C. C. Piotrowski (2012), Measuring currents in a coastal inlet by advection of turbulent eddies in airborne optical imagery, *J. Geophys. Res.*, *117*(C03020), doi:10.1029/2011JC007600.

Fairall, C. W., E. F. Bradley, J. S. Godfrey, G. A. Wick, J. B. Edson, and G. S. Young (1996), Cool-skin and warm-layer effects on sea surface temperature, *J. Geophys. Res.*, *101*(C1), 1295-1308.

Garbe, C. S., U. Schimpf, and B. Jähne (2004), A surface renewal model to analyze infrared image sequences of the ocean surface for the study of air-sea heat and gas exchange, *J. Geophys. Res.*, *109*(C08S15), doi:10.1029/2003JC001802.

Jackson, R. G. (1976), Sedimentological and fluid-dynamic implications of the turbulent bursting phenomenon in geophysical flows, *Journal of Fluid Mechanics*, *77*(03), 531-560.

Jessup, A. T., W. E. Asher, M. Atmane, K. Phadnis, C. J. Zappa, and M. R. Loewen (2009), Evidence for complete and partial surface renewal at an air-water interface, *Geophys. Res. Lett.*, *36*(L16601), doi:10.1029/2009GL038986.

Katsaros, K. B., W. T. Liu, J. A. Businger, and J. E. Tillman (1977), Heat transport and thermal structure in the interfacial boundary layer measured in an open tank of water in turbulent free convection, *Journal of Fluid Mechanics*, *83*(2), 311-335.

Korchoka, Y. (1968), Investigation of the dune movement of sediments on the Polomet River, *River. Sov. Hydrol*, 541-559.

Lucas, B. D., and T. Kanade (1981), An Iterative Image Registration Technique with an Application to Stereo Vision, *Proceedings of Imaging Understanding Workshop*, 121-130.

McKenna, S. P., and W. R. McGillis (2002), Performance of digital image velocimetry processing techniques, *Exp. Fluids*, *32*, 116-115, doi:DOI 10.1007/S003480100348.

McKenna, S. P., and W. R. McGillis (2004), The role of free-surface turbulence and surfactants in air-water gas transfer, *International Journal of Heat and Mass Transfer*, *47*, 539-553.

Rao, K. N., R. Narasimha, and M. Narayanan (1971), The 'bursting'phenomenon in a turbulent boundary layer, *Journal of Fluid Mechanics*, *48*(02), 339-352.

Saunders, P. M. (1967), The temperature at the ocean-air interface, *Journal of the Atmospheric Sciences*, *24*, 269-273.

Tennekes, H., and J. L. Lumley (1972), *A First Course in Turbulence*, MIT Press, Cambridge, Mass.

Variano, E. A., and E. A. Cowen (2008), A random-jet-stirred turbulence tank, *Journal of Fluid Mechanics*, *604*, 1-32, doi:10.1017/S0022112008000645.

Zuckerman, S., S. P. Anderson, C. J. Zappa, and R. A. Smith (2011), Infrared Observations of Temperature Modulations on the Hudson River, *AGU Fall Meeting Abstracts*, *51*, 1331.

PUBLICATIONS

Brumer, S. E., C. J. Zappa, S. P. Anderson, and J. P. Dugan (2015), Riverine Skin Temperature Response to Subsurface Processes in Low Wind Speeds, *Journal of Geophysical Research-Oceans*. [In 2nd Revision].

Brumer, S. E., C. J. Zappa, S. P. Anderson, and J. P. Dugan (2012), Using skin temperature variability to quantify surface and subsurface estuarine processes, *AGU Fall Meeting Abstracts*, *14*, 05. [Published].

Zuckerman, S., S. P. Anderson, C. J. Zappa, and R. A. Smith (2011), Infrared Observations of Temperature Modulations on the Hudson River, *AGU Fall Meeting Abstracts*, *51*, 1331. [Published].